HHS Public Access

Author manuscript

*J Am Chem Soc*. Author manuscript; available in PMC 2023 November 27.

Published in final edited form as:

*J Am Chem Soc*. 2023 February 08; 145(5): 2787–2793. doi:10.1021/jacs.2c13396.

# Late-Stage C($sp^3$)–H Methylation of Drug Molecules

**Edna Mao**,

Merck Center for Catalysis at Princeton University, Princeton, New Jersey 08544, United States

**David W.C. MacMillan**

Merck Center for Catalysis at Princeton University, Princeton, New Jersey 08544, United States

## Abstract

Methyl groups are well understood to play a critical role in pharmaceutical molecules, especially those bearing saturated heterocyclic cores. Accordingly, methods that install methyl groups onto complex molecules are highly coveted. Late-stage C–H functionalization is a particularly attractive approach, allowing chemists to bypass lengthy syntheses and facilitating the expedited synthesis of drug analogues. Herein, we disclose the direct introduction of methyl groups via C($sp^3$)–H functionalization of a broad array of saturated heterocycles, enabled by the merger of decatungstate photocatalysis and a unique nickel-mediated $S_H2$ bond formation. To further demonstrate its synthetic utility as a tool for late-stage functionalization, this method was applied to a range of drug molecules en route to an array of methylated drug analogues.

The term “magic methyl effect” has been coined to describe the significant increases in potency, efficacy, or stability that often arise when a methyl group is introduced to a pharmaceutical compound.[1,2] This effect is especially pertinent to the saturated heterocyclic cores of drugs, where a strategically placed methyl substituent can drastically transform conformational preferences, allowing for the modulation of 3D structure through a minimal disturbance in molecular weight (Figure 1).[3,4] Consequently, methyl analogues of drug candidates are high value targets in discovery campaigns.[5–8] However, generating a library of such analogues can be a significant synthetic burden, requiring multiple lengthy *de novo* syntheses. To meet these synthetic demands, late-stage functionalization has arisen as the most attractive approach for the generation and diversification of drug analogue libraries.[9–11] As such, considerable research has been devoted to the late-stage incorporation of methyl groups onto pharmaceutical scaffolds at both $sp^2$ and $sp^3$ carbon centers.[12] Recent notable efforts to install methyl groups at $\alpha$-heteroatom C($sp^3$)–H centers have broadly taken one of two approaches. First, two-step sequences have been reported, invoking C–H oxidation through an iminium or oxonium intermediate, followed by a subsequent nucleophilic methyl addition.[13,14] Alternatively, reports from our group and Stahl demonstrate one-step protocols merging nickel catalysis with light-mediated hydrogen atom transfer (HAT).[15,16] However, current technologies remain to be generalized across

**Corresponding Author**: **David W.C. MacMillan** – Merck Center for Catalysis at Princeton University, Princeton, New Jersey 08544, United States; dmacmill@princeton.edu.

Complete contact information is available at: https://pubs.acs.org/10.1021/jacs.2c13396

The authors declare the following competing financial interest(s): D.W.C.M. declares a competing financial interest with respect to the integrated photoreactor.

substrate classes and have limited application to the late-stage functionalization of drug-like molecules.

In biological systems, carbon–methyl bond formation is typically accomplished via cobalamin-dependent radical S-adenosylmethionine (SAM) methyltransferases.[17,18] Radical SAM enzymes operate by generating a 5′-deoxyadenosyl radical that performs HAT on biochemical substrates to generate a carbon-centered radical.[19,20] This open-shell species reacts with a methylcobalamin complex through a bimolecular homolytic substitution ($S_H2$) to forge C($sp^3$)-methyl bonds.[21,22] Utilizing these elementary steps, radical SAM enzymes are able to efficiently install methyl substituents onto complex and functionally dense biomolecules, such as amino acids, nucleic acids, and biosynthetic intermediates. Given the broad utility of this approach in biochemistry, we sought to employ a similar reaction design to target the late-stage C($sp^3$)–H methylation of drug molecules. The success of the envisioned reaction platform hinges on two fundamental steps: (1) alkyl radical generation via catalytic site-selective HAT and (2) $S_H2$-mediated methyl–C($sp^3$) bond formation.

In considering an appropriate catalytic HAT manifold to enact C–H methylation, we were drawn to the decatungstate anion.[23,24] Many groups, including our own, have successfully demonstrated the merger of decatungstate photocatalysis and transition metal cross-coupling for a diverse array of C–H functionalizations;[25–29] however, the application of this platform toward C($sp^3$)–C($sp^3$) coupling has yet to be explored. The excited state decatungstate enables the facile abstraction of hydridic C–H bonds; meanwhile, its size discourages abstraction at sterically hindered sites, circum-venting potential issues with overalkylation and stereocenter racemization.[30] To mediate efficient carbon–carbon bond formation, we considered $S_H2$ reactivity, which has recently emerged as a mode of reactivity for organic synthesis.[31–34] A notabe report from our group details the $S_H2$ of an alkyl radical onto an iron-porphyrin–alkyl complex as the critical elementary step to forge challenging C($sp^3$)–C($sp^3$) bonds.[35] While this bond-forming mechanism is commonly associated with metal-porphyrinoids, the Sanford lab has characterized a high valent nickel scorpionate–alkyl complex proposed to undergo $S_H2$ with aryl radicals.[36] Inspired by this work, our group has recently reported a doubly decarboxylative C($sp^3$)–C($sp^3$) coupling through radical sorting and $S_H2$, enabled by a high valent nickel-scorpionate scaffold.[37] We hypothesized that our reaction design merging photoredox-HAT and $S_H2$ catalysis can allow for broad late-stage access to methyl-bearing drug analogues.

The proposed reaction mechanism is outlined in Figure 2. Photoexcitation of decatungstate anion **1**, followed by rapid intersystem crossing, yields the excited decatungstate triplet state $*[W_{10}O_{32}]^{4-}$ (**2**).[38–43] This electrophilic species performs a polarity-matched HAT at the hydridic $\alpha$-amino C–H bond of substrate **3**. The HAT results in reduced decatungstate ($[W_{10}O_{32}]^{5-}$, **4**) as well as alkyl radical **5**. The reduced decatungstate **4** undergoes disproportionation to regenerate ground state decatungstate **1**, as well as doubly reduced decatungstate ($[W_{10}O_{32}]^{6-}$, **6**).[44] This species ($E_{1/2red}([W_{10}O^{32}]^{5-}/[W_{10}O_{32}]^{6-})$ = −1.48 V in MeCN vs SCE) performs single electron reduction of *N*-acetyloxyphthalimide (**7**, $E_{red}$ = −1.37 V in MeCN vs SCE)),[45] triggering its decarboxylation to afford methyl radical **8**, and turning over the decatungstate cycle. Methyl radical **8** is selectively sequestered by nickel complex **9**, forming complex **10** which undergoes $S_H2$ with alkyl radical **5**. This

bond-forming turns over the nickel catalyst and furnishes the C($sp^3$)–methyl product (**11**). Key to the success of this mechanism is the nickel-mediated radical sorting effect.[35,37,46] The propensity for radicals to bind **9** is inversely correlated with the degree of substitution at the radical-bearing carbon.[47] Consequently, the selective trapping of methyl radical **8** to form **10** is relatively favorable, lowering the concentration of free methyl radical in solution. Meanwhile, the binding of a 2° radical to form **12** is highly disfavored and reversible, directing the unbound **5** to couple with **10** and form the cross-coupled product **11**.

After an optimization campaign, we identified conditions in which irradiation at 365 nm light of *N*-Boc piperidine **5**, *N*-acetyloxyphthalimide **7** (2 equiv), Ni(II) acetylacetonate/KTp* (10 mol %), and tetrabutylammonium decatungstate (5 mol %) in acetone [0.1 M] for 8 h, resulted in good yields of methylated products (see Supporting Information (SI) for optimization details). We next evaluated the scope of the transformation, focusing our attention on over ten classes of prevalent saturated heterocycles in drugs (Table 1).[48–50] Four- to seven-membered azacycles underwent reaction to deliver methylated ring systems in moderate to excellent yields (**14–17**, 39–86% yield). Piperazine **18** was delivered with the methyl group $\alpha$- to the comparatively more electron-rich nitrogen (41% yield). *N*-Substituted morpholines were functionalized at the more hydridic $\alpha$-amino sites (**19**–**21**, 49% to 64% yield). Methyl groups could also be introduced to semisaturated bicycles to deliver **22** and **23** (47% and 70% yields, respectively). The piperazine cores of buspirone and terazosin were functionalized in good yields to deliver **24** (72% yield, 2:1 mono/bis-Me) and **25** (55% yield, 1:1 r.r.), respectively. The regioselectivity in cases such as these is determined by the relative hydricities of all abstractable C–H bonds. Piperidines, the most common saturated heterocycle in drug molecules, make up the cores of haloperidol, risperidone, and crizotinib. Pleasingly, the C($sp^3$)-methylations of these rings with varying 4- substitutions proceeded efficiently (**26–28**, 44%–70% yield). Notably, the benzisoxazole moiety of **27**, which typically undergoes oxidative addition into Ni(0),[51] was stable under our reaction conditions. The core of lifitegrast, a benzoyl-substituted tetrahydroquinoline, was functionalized at two $\alpha$-amino positions (**29**, 55% yield, 1:1 r.r.). In addition to nitrogen heterocycles, $\alpha$-oxy methylation could also be accomplished at lower efficiencies. A heteroaryl-fused tetrahydrofuran was functionalized at both $\alpha$-oxy sites to deliver **30** (47%, 1:1 r.r.) Five- and six-membered cyclic ethers underwent C($sp^3$)-methyl coupling in moderate yields and predictable selectivities (**31**–**34**, 31–52% yield).

We next examined the late-stage incorporation of methyl groups onto drug molecules —a longstanding goal for medicinal chemists.[52] As shown in Table 2, Boc-protected fluoxetine was functionalized preferentially at the primary site (**35**, 40%, 83% selectivity), representing a one-carbon homologation of an acyclic amine. Interestingly, a methyl group was selectively coupled onto praziquantel at the tertiary $\alpha$-amino position (**36**, 47%). This is the only example we encountered where tertiary functionalization took precedence over secondary. The unique fused structure of the drug may impart a cupped geometry onto the molecule, allowing for tertiary C–H abstraction. Furthermore, the ability to form sterically congested bonds is characteristic to $S_H2$ reactions. Methyl-leviteracetam was generated as a single regioisomer in synthetically useful yield (**37**, 25%, 1.8:1 d.r.). Clopidogrel, bearing a tertiary trialkylamine, was functionalized at both secondary $\alpha$-amino positions (**38**, 28%,

1:1 r.r.). A methyl substituent was selectively introduced onto the oxazolidinone ring of linezolid (**39**, 34%) to produce a single regioisomer and diastereomer. An analogue of a "magic methyl" compound reported by Merck[3] underwent transformation to yield both *trans* and *cis* isomers in one vessel (**40**, 54%, 4.3:1 d.r.). A methyl group was selectively incorporated onto the convex face of Boc-varenicline (**41**, 57% yield, 1.3:1 mono/bis-Me). Reaction of loratadine resulted in preferential functionalization of the $\alpha$-amino and benzylic positions, over the weaker but sterically hindered allylic positions (**42**, 49%, 67% $\alpha$-amino selectivity). Resultingly, four methylated isomers of loratadine were accessed in a single reaction. The methyl analogue of *N*-Boc-sitagliptin was generated in good yields (**43**, 66%) without any erosion of the amine stereocenter. Finally, methylation of the piperazine of olaparib proceeded in good conversions, delivering methyl substituents preferentially at the more electron-rich and sterically accessible C–H bonds (**44**, 52%).

To illustrate a potential application of this method in a drug discovery campaign, we endeavored to perform a unified, divergent synthesis of methylated drug analogues. Suvorexant, a top-selling small molecule drug for the treatment of insomnia,[53] is a representative example of the transformative effects that a methyl group can impart. In early stages, metabolism studies determined that the 7-position of the diazepane ring was susceptible to oxidation.[54] The incorporation of a methyl group at that position resulted in an increase in potency and decrease in clearance rates, improvements that culminated in the eventual approval of the methylated drug. The *des*-methyl analogue of suvorexant **(45a)** can be synthesized in two steps from commercially available reagents. Subjecting this material to reaction conditions resulted in a 62% yield of a mixture of methyl-bearing products as well as recoverable starting material. In three steps, (±)-suvorexant (**45–1**)was obtained along with all other $\alpha$-amino-methyl analogues (Table 3). We believe this example highlights this method's ability to enable the rapid synthesis methylated analogues.

In summary, we report a method for the direct C($sp^3$)–H methylation of drug-like fragments and drug compounds. We have demonstrated that a bioinspired reaction via an HAT–$S_H2$ dual catalytic strategy is an effective new platform for performing this highly coveted transformation. The stereo-electronic properties of the decatungstate catalyst allow for selective $\alpha$-heteroatom functionalization of a variety of saturated heterocycles, and the unique outer-sphere reactivity of a high-valent nickel scorpionate complex allows for mild and efficient bond formation. Overall, a variety of differentially substituted nitrogen heterocycles were tolerated under our reaction conditions (see SI for discussion and guidelines for substrate selection). We envision that this method will allow for the efficient synthesis of methylated analogues of valuable small molecules and highly expedite the exploration of the magic methyl effect.

## Supplementary Material

Refer to Web version on PubMed Central for supplementary material.

## ACKNOWLEDGMENTS

The authors are grateful for financial support provided by the National Institute of General Medical Sciences (NIGMS), the NIH (under Award No. R35GM134897-03), the Princeton Catalysis Initiative, and kind gifts from

Merck, Janssen, BMS, Genentech, Celgene, and Pfizer. The content is solely the responsibility of the authors and does not necessarily represent the official views of NIGMS. E.M. thanks Princeton University, E. Taylor, and the Taylor family for an Edward C. Taylor Fellowship. The authors thank W. Liu, P. Sarver, and N. Intermaggio for helpful scientific discussions, and R. Lambert for assistance in the preparation of this manuscript.

## REFERENCES

(1). Schönherr H; Cernak T Profound Methyl Effects in Drug Discovery and a Call for New C-H Methylation Reactions. Angew. Chem., Int. Ed 2013, 52, 12256–12267.

(2). Barreiro EJ; Kümmerle AE; Fraga CAM The Methylation Effect in Medicinal Chemistry. Chem. Rev 2011, 111, 5215–5246. [PubMed: 21631125]

(3). Coleman PJ; Schreier JD; Cox CD; Breslin MJ; Whitman DB; Bogusky MJ; McGaughey GB; Bednar RA; Lemaire W; Doran SM; Fox S. v.; Garson SL; Gotter AL; Harrell CM; Reiss DR; Cabalu TD; Cui D; Prueksaritanont T; Stevens J; Tannenbaum PL; Ball RG; Stellabott J; Young SD; Hartman GD; Winrow CJ; Renger JJ Discovery of [(2R,5R)-5-{[(5-Fluoropyridin-2-Yl) Oxy]Methyl}−2-Methylpiperidin-1-Yl][5-Methyl-2-(Pyrimidin-2-Yl) Phenyl]Methanone (MK-6096): A Dual Orexin Receptor Antagonist with Potent Sleep-Promoting Properties. ChemMedChem. 2012, 7, 415–424. [PubMed: 22307992]

(4). Piotrowski DW; Futatsugi K; Casimiro-Garcia A; Wei L; Sammons MF; Herr M; Jiao W; Lavergne SY; Coffey SB; Wright SW; Song K; Loria PM; Banker ME; Petersen DN; Bauman J Identification of Morpholino-2H-Pyrido[3,2-b][1,4]-Oxazin-3(4H)-Ones as Nonsteroidal Mineralocorticoid Antagonists. J. Med. Chem 2018, 61, 1086–1097. [PubMed: 29300474]

(5). Letavic MA; Savall BM; Allison BD; Aluisio L; Andres JI; de Angelis M; Ao H; Beauchamp DA; Bonaventure P; Bryant S; Carruthers NI; Ceusters M; Coe KJ; Dvorak CA; Fraser IC; Gelin CF; Koudriakova T; Liang J; Lord B; Lovenberg TW; Otieno MA; Schoetens F; Swanson DM; Wang Q; Wickenden AD; Bhattacharya A 4-Methyl-6,7-Dihydro-4H-Triazolo[4,5-c]Pyridine-Based P2 × 7 Receptor Antagonists: Optimization of Pharmacokinetic Properties Leading to the Identification of a Clinical Candidate. J. Med. Chem 2017, 60, 4559–4572. [PubMed: 28493698]

(6). Foote KM; Nissink JWM; McGuire T; Turner P; Guichard S; Yates JWT; Lau A; Blades K; Heathcote D; Odedra R; Wilkinson G; Wilson Z; Wood CM; Jewsbury PJ Discovery and Characterization of AZD6738, a Potent Inhibitor of Ataxia Telangiectasia Mutated and Rad3 Related (ATR) Kinase with Application as an Anticancer Agent. J. Med. Chem 2018, 61, 9889–9907. [PubMed: 30346772]

(7). Kettle JG; Bagal SK; Bickerton S; Bodnarchuk MS; Breed J; Carbajo RJ; Cassar DJ; Chakraborty A; Cosulich S; Cumming I; Davies M; Eatherton A; Evans L; Feron L; Fillery S; Gleave ES; Goldberg FW; Harlfinger S; Hanson L; Howard M; Howells R; Jackson A; Kemmitt P; Kingston JK; Lamont S; Lewis HJ; Li S; Liu L; Ogg D; Phillips C; Polanski R; Robb G; Robinson D; Ross S; Smith JM; Tonge M; Whiteley R; Yang J; Zhang L; Zhao X Structure-Based Design and Pharmacokinetic Optimization of Covalent Allosteric Inhibitors of the Mutant GTPase $KRAS^{g12c}$. J. Med. Chem 2020, 63, 4468–4483. [PubMed: 32023060]

(8). Brebion F; Gosmini R; Deprez P; Varin M; Peixoto C; Alvey L; Jary H; Bienvenu N; Triballeau N; Blanque R; Cottereaux C; Christophe T; Vandervoort N; Mollat P; Touitou R; Leonard P; De Ceuninck F; Botez I; Monjardet A; van der Aar E; Amantini D Discovery of GLPG1972/S201086, a Potent, Selective, and Orally Bioavailable ADAMTS-5 Inhibitor for the Treatment of Osteoarthritis. J. Med. Chem 2021, 64, 2937–2952. [PubMed: 33719441]

(9). Cernak T; Dykstra KD; Tyagarajan S; Vachal P; Krska SW The Medicinal Chemist's Toolbox for Late Stage Functionalization of Drug-like Molecules. Chem. Soc. Rev 2016, 45, 546–576. [PubMed: 26507237]

(10). Börgel J; Ritter T Late-Stage Functionalization. Chem. 2020, 6, 1877–1887.

(11). Guillemard L; Kaplaneris N; Ackermann L; Johansson MJ Late-Stage C-H Functionalization Offers New Opportunities in Drug Discovery. Nat. Rev. Chem 2021, 5, 522–545. [PubMed: 37117588]

(12). Aynetdinova D; Callens MC; Hicks HB; Poh CYX; Shennan BDA; Boyd AM; Lim ZH; Leitch JA; Dixon DJ Installing the "magic Methyl" - C-H Methylation in Synthesis. Chem. Soc. Rev 2021, 50, 5517–5563. [PubMed: 33690769]

(13). Feng K; Quevedo RE; Kohrt JT; Oderinde MS; Reilly U; White MC Late-Stage Oxidative C($sp^3$)-H Methylation. Nature 2020, 580, 621–627. [PubMed: 32179876]

(14). Novaes LFT; Ho JSK; Mao K; Liu K; Tanwar M; Neurock M; Villemure E; Terrett JA; Lin S Exploring Electrochemical C($sp^3$)-H Oxidation for the Late-Stage Methylation of Complex Molecules. J. Am. Chem. Soc 2022, 144, 1187–1197. [PubMed: 35015533]

(15). Le C; Liang Y; Evans RW; Li X; Macmillan DWC Selective $sp^3$ C-H Alkylation via Polarity-Match-Based Cross-Coupling. Nature 2017, 547, 79–83. [PubMed: 28636596]

(16). Vasilopoulos A; Krska SW; Stahl SS C($sp^3$)-H Methylation Enabled by Peroxide Photosensitization and Ni-Mediated Radical Coupling. Science 2021, 372, 398–403. [PubMed: 33888639]

(17). Broderick JB; Duffus BR; Duschene KS; Shepard EM Radical S-Adenosylmethionine Enzymes. Chem. Rev 2014, 114, 4229–4317. [PubMed: 24476342]

(18). Fujimori DG Radical SAM-Mediated Methylation Reactions. Curr. Opin. Chem. Biol 2013, 17, 597–604. [PubMed: 23835516]

(19). Bauerle MR; Schwalm EL; Booker SJ Mechanistic Diversity of Radical S-Adenosylmethionine (SAM)-Dependent Methylation. J. Biol. Chem 2015, 290, 3995–4002. [PubMed: 25477520]

(20). Zhang QI; van der Donk WA; Liu W Radical-Mediated Enzymatic Methylation: A Tale of Two SAMS. Acc. Chem. Res 2012, 45, 555–564. [PubMed: 22097883]

(21). Wang Y; Begley TP Mechanistic Studies on CysS - A Vitamin B12-Dependent Radical SAM Methyltransferase Involved in the Biosynthesis of the Tert-Butyl Group of Cystobactamid. J. Am. Chem. Soc 2020, 142, 9944–9954. [PubMed: 32374991]

(22). Halpern J Mechanisms of Coenzyme B12-Dependent Rearrangements. Science 1985, 227, 869–875. [PubMed: 2857503]

(23). Capaldo L; Quadri LL; Ravelli D Photocatalytic Hydrogen Atom Transfer: The Philosopher's Stone for Late-Stage Functionalization? Green Chem. 2020, 22, 3376–3396.

(24). Tzirakis MD; Lykakis IN; Orfanopoulos M Decatungstate as an Efficient Photocatalyst in Organic Chemistry. Chem. Soc. Rev 2009, 38, 2609–2621. [PubMed: 19690741]

(25). Perry IB; Brewer TF; Sarver PJ; Schultz DM; DiRocco DA; MacMillan DWC Direct Arylation of Strong Aliphatic C-H Bonds. Nature 2018, 560, 70–75. [PubMed: 30068953]

(26). West JG; Huang D; Sorensen EJ Acceptorless Dehydrogenation of Small Molecules through Cooperative Base Metal Catalysis. Nat. Commun 2015, 6, 1–7.

(27). Sarver PJ; Bacauanu V; Schultz DM; DiRocco DA; Lam Y.-h.; Sherer EC; MacMillan DWC The Merger of Decatungstate and Copper Catalysis to Enable Aliphatic C($sp^3$)-H Trifluoromethylation. Nat. Chem 2020, 12, 459–467. [PubMed: 32203440]

(28). Fan P; Lan Y; Zhang C; Wang C Nickel/Photo-Cocatalyzed Asymmetric Acyl-Carbamoylation of Alkenes. J. Am. Chem. Soc 2020, 142, 2180–2186. [PubMed: 31971787]

(29). Wang L; Wang T; Cheng GJ; Li X; Wei JJ; Guo B; Zheng C; Chen G; Ran C; Zheng C Direct C-H Arylation of Aldehydes by Merging Photocatalyzed Hydrogen Atom Transfer with Palladium Catalysis. ACS Catal. 2020, 10, 7543–7551.

(30). Ravelli D; Fagnoni M; Fukuyama T; Nishikawa T; Ryu I Site-Selective C-H Functionalization by Decatungstate Anion Photo-catalysis: Synergistic Control by Polar and Steric Effects Expands the Reaction Scope. ACS. Catal 2018, 8, 701–713.

(31). Wang Y; Wen X; Cui X; Zhang XP Enantioselective Radical Cyclization for Construction of 5-Membered Ring Structures by Metalloradical C-H Alkylation. J. Am. Chem. Soc 2018, 140, 4792–4796. [PubMed: 29584958]

(32). Zhou M; Lankelma M; van der Vlugt JI; de Bruin B Catalytic Synthesis of 8-Membered Ring Compounds via Cobalt(III)-Carbene Radicals. Angew. Chem., Int. Ed 2020, 59, 11073–11079.

(33). Xie J; Xu P; Zhu Y; Wang J; Lee WCC; Zhang XP New Catalytic Radical Process Involving 1,4-Hydrogen Atom Abstraction: Asymmetric Construction of Cyclobutanones. J. Am. Chem. Soc 2021, 143, 11670–11678. [PubMed: 34292709]

(34). Wang X; Ke J; Zhu Y; Deb A; Xu Y; Zhang XP Asymmetric Radical Process for General Synthesis of Chiral Heteroaryl Cyclopropanes. J. Am. Chem. Soc 2021, 143, 11121–11129. [PubMed: 34282613]

(35). Liu W; Lavagnino MN; Gould CA; Alcázar J; MacMillan DWC A Biomimetic SH2 Cross-Coupling Mechanism for Quaternary $sp^3$-Carbon Formation. Science 2021, 374, 1258–1263. [PubMed: 34762491]

(36). Bour JR; Ferguson DM; Mcclain EJ; Kampf JW; Sanford MS Connecting Organometallic Ni(III) and Ni(IV): Reactions of Carbon-Centered Radicals with High-Valent Organo-nickel. J. Am. Chem. Soc 2019, 141, 8914–8920. [PubMed: 31136162]

(37). Tsymbal AV; Bizzini LD; MacMillan DWC Nickel Catalysis via SH2 Homolytic Substitution: The Double Decarboxylative Cross-Coupling of Aliphatic Acids. J. Am. Chem. Soc 2022, 144, 21278–21286. [PubMed: 36375080]

(38). De Waele V; Poizat O; Fagnoni M; Bagno A; Ravelli D Unraveling the Key Features of the Reactive State of Decatungstate Anion in Hydrogen Atom Transfer (HAT) Photocatalysis. ACS Catal. 2016, 6, 7174–7182.

(39). Ravelli D; Dondi D; Fagnoni M; Albini A; Bagno A Electronic and EPR Spectra of the Species Involved in $[W_{10}O_{32}]^{4-}$ Photocatalysis. A Relativistic DFT Investigation. Phys. Chem. Chem. Phys 2013, 15, 2890–2896. [PubMed: 23338044]

(40). Tanielian C; Lykakis IN; Seghrouchni R; Cougnon F; Orfanopoulos M Mechanism of Decatungstate Photocatalyzed Oxygenation of Aromatic Alcohols: Part I. Continuous Photolysis and Laser Flash Photolysis Studies. J. Mol. Catal. A Chem 2007, 262, 170–175.

(41). Texier I; Delaire JA; Giannotti C Reactivity of the Charge Transfer Excited State of Sodium Decatungstate at the Nanosecond Time Scale. Phys. Chem. Chem. Phys 2000, 2, 1205–1212.

(42). Duncan DC; Fox MA Early Events in Decatungstate Photocatalyzed Oxidations: A Nanosecond Laser Transient Absorbance Reinvestigation. J. Phys. Chem. A 1998, 102, 4559–4567.

(43). Duncan DC; Netzel TL; Hill CL Early-Time Dynamics and Reactivity of Polyoxometalate Excited States. Identification of a Short-Lived LMCT Excited State and a Reactive Long-Lived Charge-Transfer Intermediate Following Picosecond Flash Excitation of $[W_{10}O_{32}]^{4-}$ in Acetonitrile. Inorg. Chem 1995, 34, 4640–4646.

(44). Yamase T; Usami T Photocatalytic Dimerization of Olefins by Decatungstate(VI), $[W_{10}O_{32}]^{4-}$, in Acetonitrile and Magnetic Resonance Studies of Photoreduced Species. J. Chem. Soc., Dalt. Trans 1988, 1, 183–190.

(45). Okada K; Okamoto K; Oda M A New and Practical Method of Decarboxylation: Photosensitized Decarboxylation of N-Acyloxyphthalimides via Electron-Transfer Mechanism. J. Am. Chem. Soc 1988, 110, 8736–8738.

(46). Sakai HA; Macmillan DWC Nontraditional Fragment Couplings of Alcohols and Carboxylic Acids: $C(sp^3)$-$C(sp^3)$ Cross-Coupling via Radical Sorting. J. Am. Chem. Soc 2022, 144, 6185–6192. [PubMed: 35353531]

(47). Simões JAM; Beauchamp JL Transition Metal-Hydrogen and Metal-Carbon Bond Strengths: The Keys to Catalysis. Chem. Rev 1990, 90, 629–688.

(48). Vitaku E; Smith DT; Njardarson JT Analysis of the Structural Diversity, Substitution Patterns, and Frequency of Nitrogen Heterocycles among U.S. FDA Approved Pharmaceuticals. J. Med. Chem 2014, 57, 10257–10274. [PubMed: 25255204]

(49). Shearer J; Castro JL; Lawson ADG; Maccoss M; Taylor RD Rings in Clinical Trials and Drugs: Present and Future. J. Med. Chem 2022, 65, 8699–8712. [PubMed: 35730680]

(50). Singh PK; Silakari O The Current Status of O-Heterocycles: A Synthetic and Medicinal Overview. ChemMedChem. 2018, 13, 1071–1087. [PubMed: 29603634]

(51). Bogdos MK; Müller P; Morandi B Structural Evidence for Aromatic Heterocycle N-O Bond Activation via Oxidative Addition. Organometallics 2023, Article ASAP. DOI: 10.1021/acs.organo-met.2c00533.

(52). Boström J; Brown DG; Young RJ; Keserü GM Expanding the Medicinal Chemistry Synthetic Toolbox. Nat. Rev. Drug Discovery 2018, 17, 709–727. [PubMed: 30140018]

(53). Qureshi MH; Williams R; Marshall C; Njardarson JT Top 200 Small Molecule Pharmaceuticals by Retail Sales in 2021. 2021. https://njardarson.lab.arizona.edu/sites/njardarson.lab.arizona.edu/files/ToT%20200%20Small%20Molecules%202021V3.pdf (accessed 2023-01-09).

(54). Cox CD; Breslin MJ; Whitman DB; Schreier JD; McGaughey GB; Bogusky MJ; Roecker AJ; Mercer SP; Bednar RA; Lemaire W; Bruno JG; Reiss DR; Harrell CM; Murphy KL;

Garson SL; Doran SM; Prueksaritanont T; Anderson WB; Tang C; Roller S; Cabalu TD; Cui D; Hartman GD; Young SD; Koblan KS; Winrow CJ; Renger JJ; Coleman PJ Discovery of the Dual Orexin Receptor Antagonist [(7R)-4-(5-Chloro-1,3-Benzoxazol-2-yl)-7-Methyl-1,4-Diazepan-1-yl][5-Methyl-2-(2H-1,2,3-Triazol-2-yl) Phenyl]Methanone (MK-4305) for the Treatment of Insomnia. J. Med. Chem 2010, 53, 5320–5332. [PubMed: 20565075]

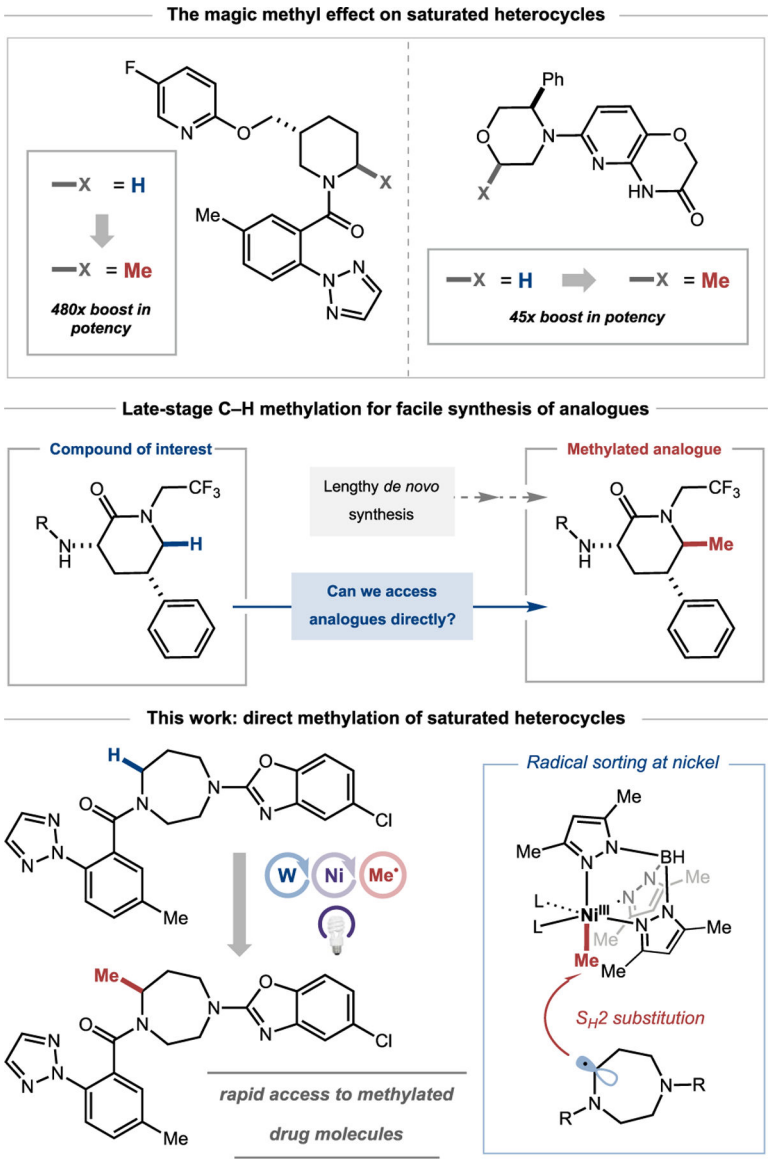


**Figure 1.**
Magic Methyl Effect.

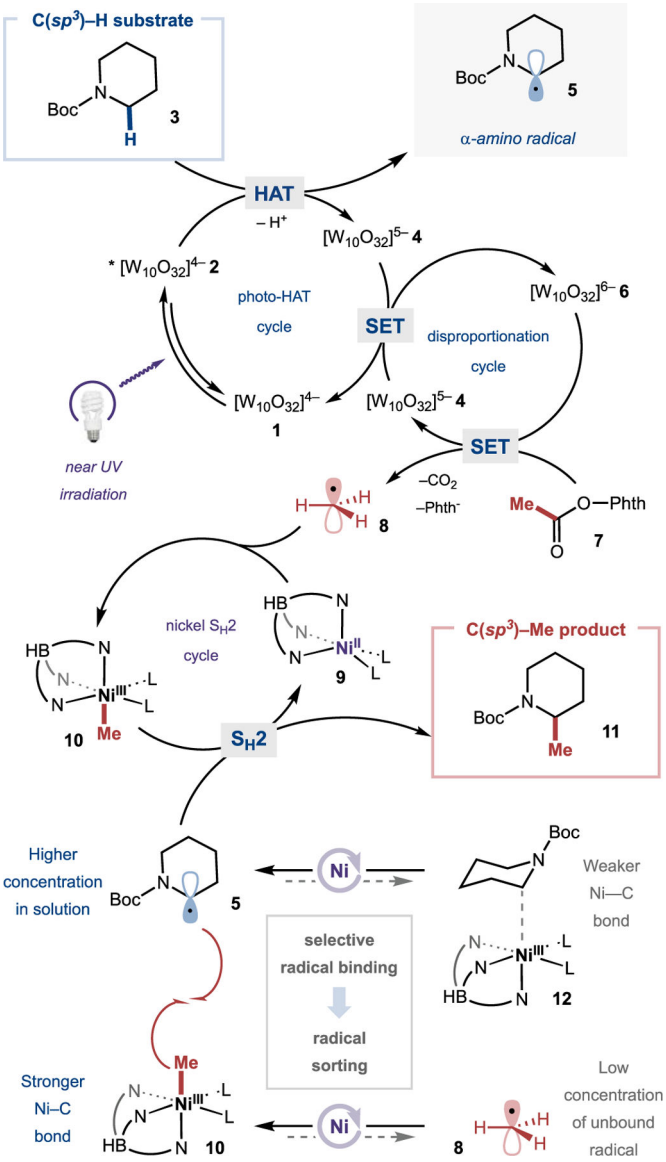


**Figure 2.**
Proposed mechanism of methylation and radical sorting.

**Table 1.**

Scope of Heterocyclic Fragments and Drug Cores[a]

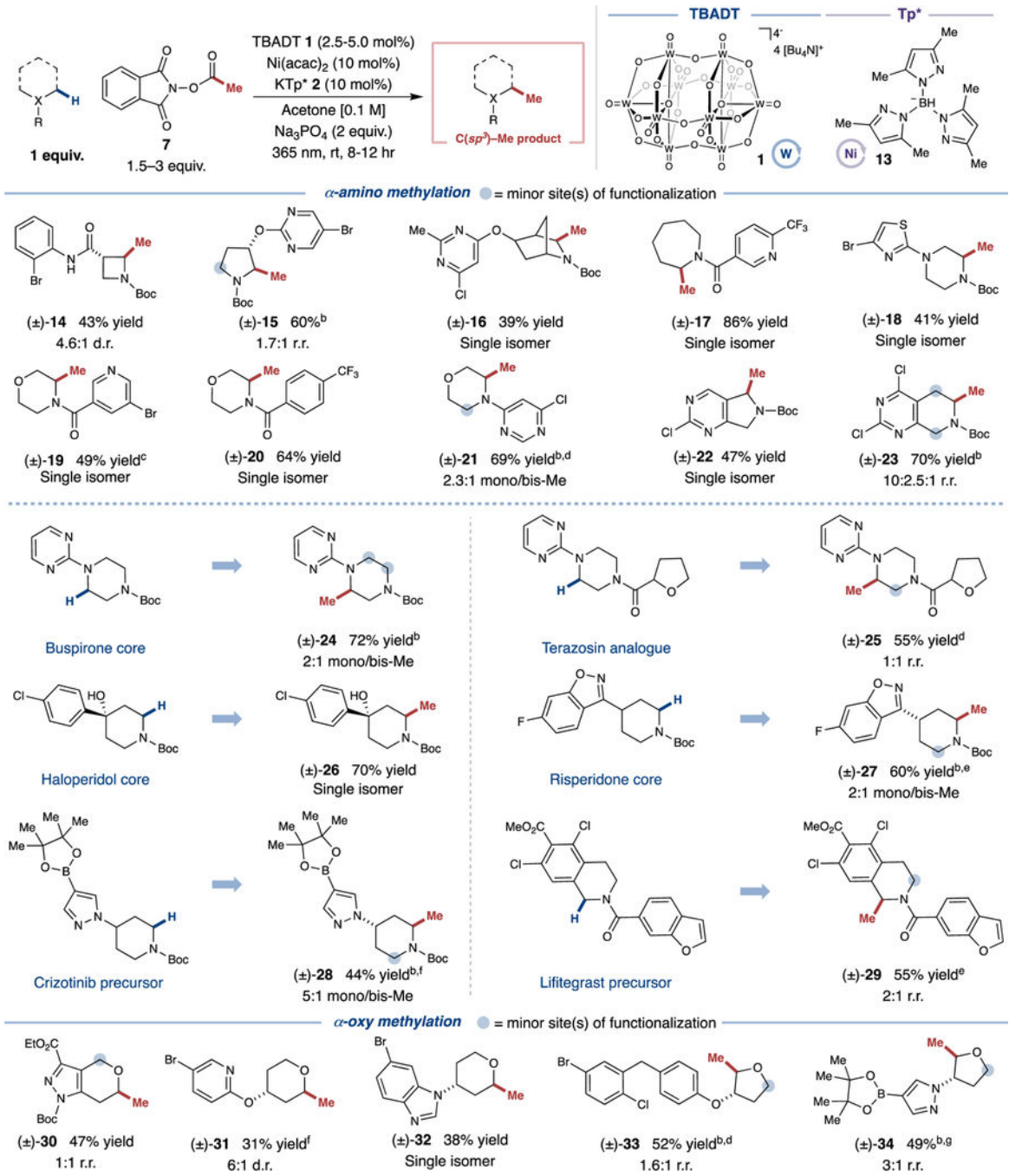


J Am Chem Soc. Author manuscript; available in PMC 2023 November 27.

[a]Yields isolated unless indicated. “Single isomer” refers to substrates for which >95% selectivity for indicated regioisomer and/or diastereomer was observed. Performed on 0.5 mmol scale with substrate (1.0 equiv), *N*-acetyloxyphthalimide (2.0 equiv), TBADT (5 mol %), $Ni(acac)_2$ (10 mol %), KTp* (10 mol %), $Na_3PO_4$ (2 equiv), acetone [0.025 M], integrated photoreactor (365 nm, 100% light intensity, 12 h).

[b]See SI for structural assignment of minor product(s).

[c]Iterative addition protocol of TBADT and/or *N*-acetyloxyphthalimide utilized. See SI for specific experimental details.

[d]2.5 mol % TBADT and 1.5 equiv of *N*-acetyloxyphthalimide used, irradiated for 8 h.

[e]4.3:1 d.r. mono-Me

[f]4:1 d.r. mono-Me

[g]Due to product instability, the assay yield is reported, which is determined by uHPLC analysis of crude reaction mixture.

**Table 2.**

Late-Stage Functionalization of Drug Molecules[a]

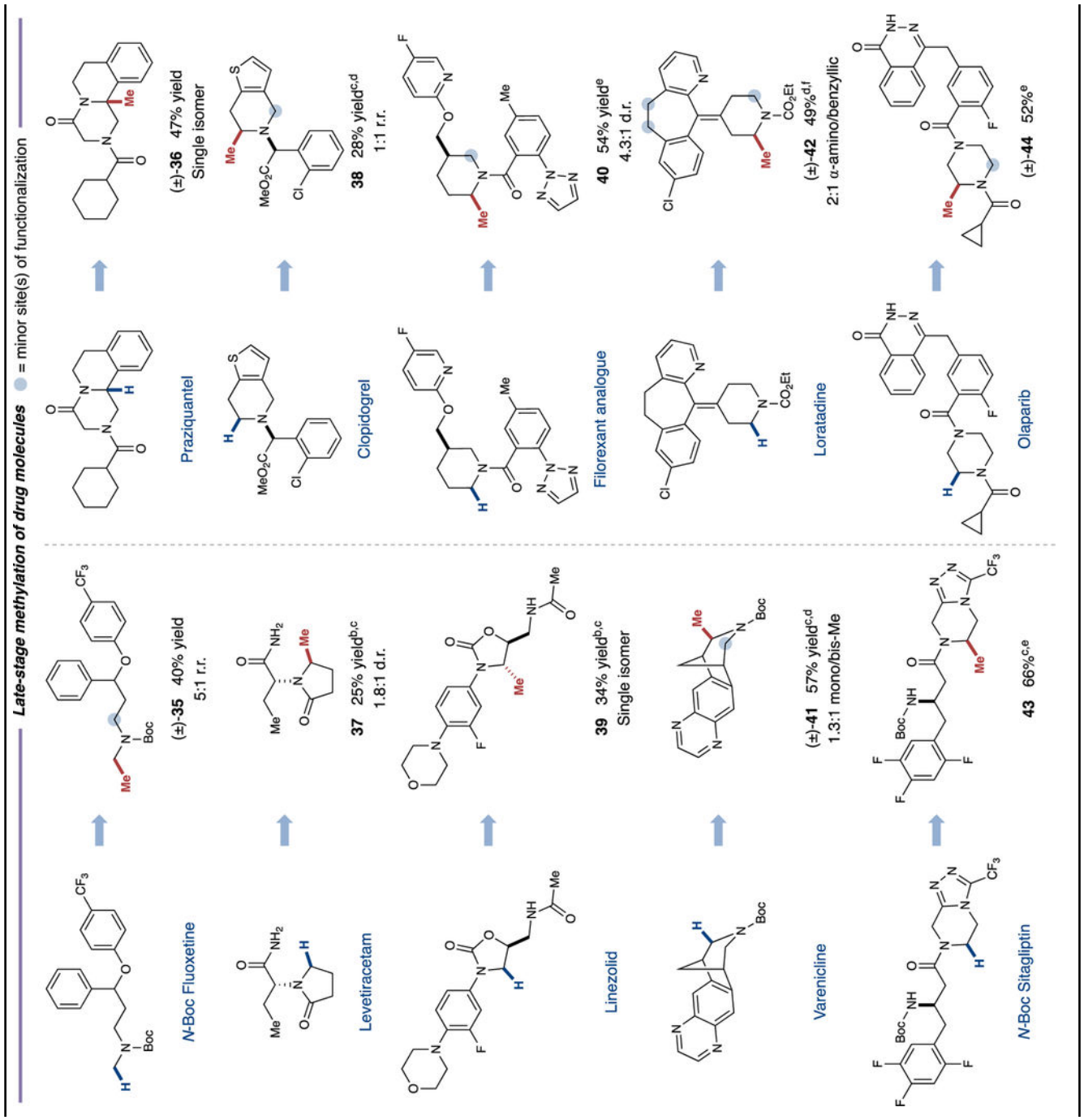

[a] Yields isolated unless indicated. “Single isomer” refers to substrates for which >95% selectivity for indicated regioisomer and/or diastereomer was observed. Performed on 0.5 mmol scale with substrate (1.0 equiv), *N*-acetyloxyphthalimide (2.0 equiv), TBADT (5 mol %), $Ni(acac)_2$ (10 mol %), KTp* (10 mol %), $Na_3PO_4$ (2 equiv), acetone [0.025 M], integrated photoreactor (365 nm, 100% light intensity, 12 h).

[b] Iterative addition protocol of TBADT and/or *N*-acetyloxyphthalimide utilized. See SI for specific experimental details.

[c] See SI for discussion of stereocenters.

[d] See SI for structural assignments of minor product(s).

[e] Minor product(s) isolated but structure(s) unassigned. Not included in reported yield. See SI for details.

[f] 2.5 mol % TBADT and 1.5 equiv of *N*-acetyloxyphthalimide used, irradiated for 8 h.

**Table 3.**

Expedited Synthesis of Suvorexant and Its Analogues[a]

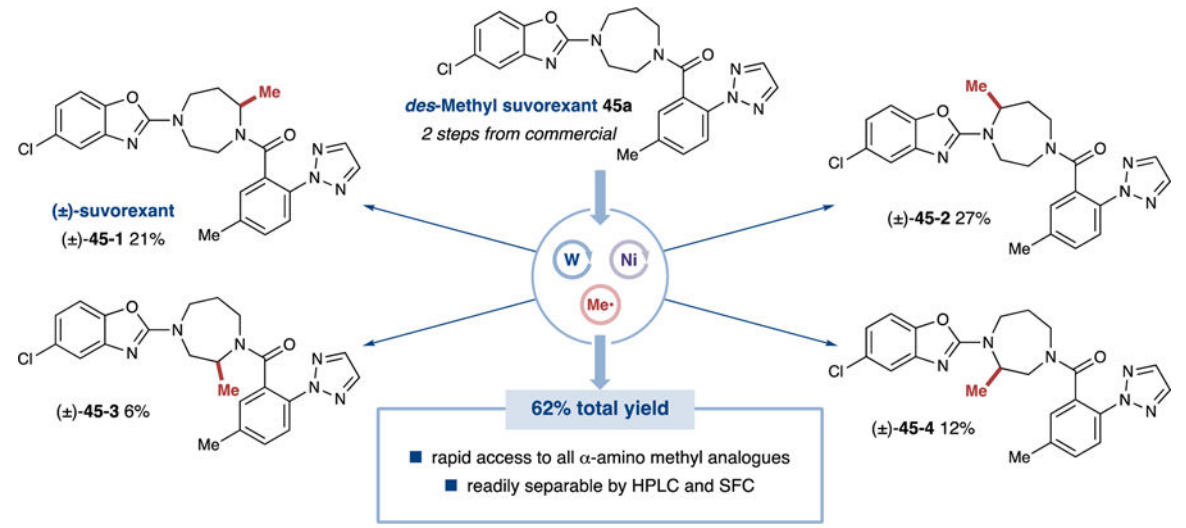


[a]All yields isolated. Performed on 0.5 mmol scale with **45a** (1.0 equiv), *N*-acetyloxyphthalimide (2.0 equiv), TBADT (5 mol %), $Ni(acac)_2$ (10 mol %), KTp* (10 mol %), $Na_3PO_4$ (2 equiv), acetone [0.05 M], integrated photoreactor (365 nm, 100% light intensity, 12 h).